Development 127, 2143-2154 (2000)
Printed in Great Britain © The Company of Biologists Limited 2000
DEV9708

Processing of the *Drosophila* Sog protein creates a novel BMP inhibitory activity

Kweon Yu[1,*], Shaila Srinivasan[1,*], Osamu Shimmi[2,*], Brian Biehs[1], Kay E. Rashka[3], David Kimelman[4], Michael B. O'Connor[2] and Ethan Bier[1,‡]

[1]Department of Biology and Center for Molecular Genetics, University of California, San Diego, La Jolla, California 92093-0349, USA
[2]Department of Genetics and Cell Biology, University of Minnesota, Minneapolis, MN 55455, USA
[3]Department of Anatomy, University of Wisconsin Medical School, Madison, WI 53706, USA
[4]Department of Biochemistry, Box 357350, University of Washington, Seattle, WA 98195-7350, USA
*These authors contributed equally to this paper
‡Author for correspondence (e-mail: bier@biomail.ucsd.edu)

Accepted 3 March; published on WWW 18 April 2000

SUMMARY

Structurally unrelated neural inducers in vertebrate and invertebrate embryos have been proposed to function by binding to BMP4 or Dpp, respectively, and preventing these homologous signals from activating their receptor(s). In this study, we investigate the functions of various forms of the *Drosophila* Sog protein using the discriminating assay of *Drosophila* wing development. We find that misexpression of *Drosophila* Sog, or its vertebrate counterpart Chordin, generates a very limited vein-loss phenotype. This *sog* misexpression phenotype is very similar to that of viable mutants of *glass-bottom boat* (*gbb*), which encodes a BMP family member. Consistent with Sog selectively interfering with Gbb signaling, Sog can block the effect of misexpressing Gbb, but not Dpp in the wing. In contrast to the limited BMP inhibitory activity of Sog, we have identified carboxy-truncated forms of Sog, referred to as Supersog, which when misexpressed cause a broad range of *dpp*$^-$ mutant phenotypes. In line with its phenotypic effects, Supersog can block the effects of both misexpressing Dpp and Gbb in the wing. Vertebrate Noggin, on the other hand, acts as a general inhibitor of Dpp signaling, which can interfere with the effect of overexpressing Dpp, but not Gbb. We present evidence that Sog processing occurs in vivo and is biologically relevant. Overexpression of intact Sog in embryos and adult wing primordia leads to the developmentally regulated processing of Sog. This in vivo processing of Sog can be duplicated in vitro by treating Sog with a combination of the metalloprotease Tolloid (Tld) plus Twisted Gastrulation (Tsg), another extracellular factor involved in Dpp signaling. In accord with this result, coexpression of intact Sog and Tsg in developing wings generates a phenotype very similar to that of Supersog. Finally, we provide evidence that *tsg* functions in the embryo to generate a Supersog-like activity, since Supersog can partially rescue *tsg*$^-$ mutants. Consistent with this finding, *sog*$^-$ and *tsg*$^-$ mutants exhibit similar dorsal patterning defects during early gastrulation. These results indicate that differential processing of Sog generates a novel BMP inhibitory activity during development and, more generally, that BMP antagonists play distinct roles in regulating the quality as well as the magnitude of BMP signaling.

Key words: *short gastrulation* (*sog*), *supersog*, *decapentaplegic* (*dpp*), BMP antagonist, Wing development, *Drosophila*

INTRODUCTION

Secreted factors in the BMP subfamily of TGFβ-related ligands play a prominent role during many phases of metazoan development. In *Drosophila*, the *decapentaplegic* (*dpp*) gene (Padgett et al., 1987), which encodes a product most related to the vertebrate BMP2 and BMP4 proteins, is involved in several aspects of patterning the embryo and adult (Segal and Gelbart, 1985). For example, during embryonic development, *dpp* is essential for formation of the dorsal-ventral (D/V) axis (Irish and Gelbart, 1987; Ray et al., 1991; Arora and Nüsslein-Volhard, 1992; Wharton et al., 1993), subdivision of the mesoderm into somatic versus visceral or cardiac components (Panganiban et al., 1990; Hursch et al., 1993; Thuringer et al., 1993), induction between the visceral mesoderm and underlying endoderm in the developing gut (Staehling-Hampton et al., 1994; Frasch, 1995), and formation of trachea (Wappner et al., 1997). During adult development *dpp* is involved in growth of imaginal discs (Campbell et al., 1993), patterning the anterior-posterior axis of imaginal discs such as the wing (Capdevila and Guerrero, 1994; Nellen et al., 1996; Lecuit et al., 1996), propagation of the morphogenetic furrow in the eye (Heberlein et al., 1993; Ma et al., 1993), development of antennal structures (Segal and Gelbart, 1985),

optic lobe development (Kaphingst and Kunes, 1994), oogenesis (Twombly et al., 1996) and wing vein development in early pupae (Yu et al., 1996). In addition to *dpp*, two other genes, *screw* (Arora et al., 1994) and *glass-bottom-boat* (*gbb*)/*60A* (Chen et al., 1998; Khalsa et al., 1998; Haerry et al., 1998), encode BMP family members that function in concert with Dpp during certain developmental stages. Scw potentiates Dpp signaling during early D/V patterning of the embryo (Arora et al., 1994) and Gbb plays an analogous role during development of adult structures such as the wing (Khalsa et al., 1998; Haerry et al., 1998).

Given the wide spectrum of developmental events controlled by Dpp/BMP signaling, it is important to know how this signaling pathway is regulated in different developmental contexts. One known mechanism for regulating BMP signaling is through inhibition by extracellular antagonists. In *Drosophila*, the *short gastrulation* (*sog*) gene has been shown to encode an extracellular Dpp antagonist (Sog) (François et al., 1994), which opposes Dpp signaling during early D/V patterning of the embryo (Ferguson and Anderson, 1992; François et al., 1994; Biehs et al., 1996) and wing vein development (Yu et al., 1996). In the case of the early embryo, Sog is expressed in the lateral neuroectoderm (François et al., 1994) and Dpp is expressed in adjacent non-neural dorsal cells. Sog functions in two capacities during this stage. First, Sog prevents Dpp signaling from spreading into the neuroectoderm by blocking an invasive positive feedback loop created by the combination of Dpp diffusing and activating its own expression (Biehs et al., 1996; Bier, 1997). Second, Sog has been proposed to diffuse into the dorsal region of the embryo where it is degraded by Tolloid (Tld), a metalloprotease expressed in dorsal cells (Marques et al., 1997). The combination of Sog expression in the lateral neuroectoderm and Tld degradation of Sog dorsally is thought to provide a source and sink configuration required for creating a concentration gradient of Sog in the dorsal region. This gradient of Sog is hypothesized to create a reciprocal asymmetry in Dpp signaling that is necessary for subdividing the dorsal region into two domains: amnioserosa (dorsalmost cells) and dorsal ectoderm (ventral portion of dorsal region) (Ferguson and Anderson, 1992; François et al., 1994; Biehs et al., 1996; Marques et al., 1997).

Chordin, the vertebrate counterpart of Sog (Sasai et al., 1994; François and Bier, 1995), and the structurally distinct vertebrate BMP antagonist Noggin (Smith and Harland, 1992) are both produced in the Spemann organizer and function analogously to Sog by inhibiting BMP4 signaling in the neural domain of early *Xenopus* embryos. These vertebrate antagonists have been shown to bind BMPs (Piccolo et al., 1996; Zimmerman et al., 1996), which presumably prevents these ligands from activating their receptors. Sog and Chordin inhibit Dpp/BMP signaling in the neuroectoderm of invertebrate and vertebrate embryos by a mechanism which has been highly conserved during the course of evolution (Padgett et al., 1993; François and Bier, 1995; Holley et al., 1995; Sasai et al., 1995; Schmidt et al., 1995; Wilson and Hemmati-Brivanlou, 1995; Biehs et al., 1996; Hammerschmidt et al., 1996; Bier, 1997; Hemmati-Brivanlou and Melton, 1997).

In this study, we examine the ability of different forms of Sog to block Dpp signaling during adult development. We focus our analysis on wing development, which depends on at least three distinct actions of Dpp signaling: wing growth, anterior-posterior (A/P) patterning and vein development. We observe that misexpression of different forms of Sog or the vertebrate BMP antagonist Noggin results in distinct wing phenotypes. We provide evidence that these differences arise from antagonists selectively interfering with the activity of particular subsets of BMPs. Sog only inhibits signaling mediated by Gbb during wing vein development. In contrast to intact Sog, truncated forms of Sog, which we refer to as Supersog, block Dpp signaling in a wide range of developmental contexts and can block the effects of misexpressing both Dpp and Gbb. Noggin is also a broadly active BMP antagonist, and can block the effect of overexpressing Dpp, but not Gbb. Sog processing is likely to be biologically relevant since N-terminal fragments of Sog that overlap with Supersog are produced in vivo in a developmentally regulated fashion. Furthermore, we show that Sog can be processed similarly in vitro by the Tld protease when an extracellular cofactor encoded by the *twisted gastrulation* (*tsg*) gene is present. Tsg plays a role in Dpp signaling in early embryos (Mason et al., 1994) and is produced in dorsal cells of the blastoderm embryo. We show that tsg^- mutants exhibit defects in patterning the dorsal region of the embryo similar to those of sog^- mutants, and that tsg^- mutant embryos can be significantly rescued by expression of Supersog but not Sog. In further support of an in vivo role for Supersog-like molecules, coexpression of intact Sog and Tsg induces Supersog-like phenotypes in the wing. We discuss these results in terms of models in which different BMP antagonists and processed forms of Sog interfere with the activities of selected subsets of BMP ligands.

MATERIALS AND METHODS

Fly stocks

Several independent lines of each *pUAS* construct were obtained by P-element mediated germline transformation. *dpp-GAL4* lines were kindly provided by Larry Zipursky (UCLA). The 8× *HS-dpp* line (embryos carrying eight copies of an *HS-dpp* construct) was kindly provided by Ron Blackman (Chemgenics, Boston) and the 8× *HS-sog* stock has been described previously (Biehs et al., 1996). Other strains carrying genetic markers or chromosome balancers were obtained from either the Bloomington, Indiana or Bowling Green, Ohio *Drosophila* stock centers.

Generation of misexpression constructs

cDNAs encoding the full coding regions of *sog*, *chordin* and *noggin* were inserted into the *pUAS* expression vector using appropriate restriction sites (Brand and Perrimon, 1993). Construction protocols of Tld-HA and Dpp-HA have been previously described (Marques et al., 1997). Tsg-His was made by insertion of 6× His epitope (MRGSHHHHHHEF) into the *Eco*RI site, which was made after Phe-248 of Tsg. Specifics of these constructs will be provided upon request.

Immunoblotting

Embryos were collected from grape juice/agar plates, dechorionated in 50% bleach solution, rinsed extensively with water, blotted dry and homogenized in 2× SDS sample buffer (100 mM Tris, pH 6.8, 200 mM DTT, 4% SDS, 20% glycerol, 0.2% Bromophenol Blue). Protein samples were boiled for 5 minutes, electrophoresed on 10% SDS-PAGE gels or 7.5%-15% gradient gels, and transferred to PVDF membranes (Bio-Rad Laboratories) using 0.1% SDS in the transfer buffer. Blots were blocked in 5% NFDM (non-fat dried milk),

incubated in primary antibody (anti-Sog 8A at 1:500 dilution) followed by incubation in secondary antibody (HRP-conjugated goat anti-rabbit (Sigma) at 1:2000 dilution), and developed using ECL (SuperSignal, Pierce or Amersham) according to the manufacturer's instructions. The A-14 rabbit polyclonal anti-Myc antibody (Santa Cruz Biotechnology) was used as a primary antibody.

Cells and protein expression

Drosophila S2 cells were grown in M3 insect medium (Sigma) with 10% IMS (insect medium supplement, Sigma). The DNA samples for Sog-Myc, Dpp-HA, Tsg-His or Tld-HA were cotransfected with pH8CO containing the methotrexate-resistant DHFR gene (ratio of 10:1). The S2 cells expressing Sog-Myc, Dpp-HA, Tsg-His or Tld-HA were selected in the medium containing 5×10^{-7} M methotrexate (Sigma) (Bunch et al., 1988). Transfections were carried out as described by Han (1996). The production of relevant proteins was induced by addition of M3 medium with 10% IMS containing 700 μg/ml $CuSO_4$. After 48 hours, the conditioned medium was collected. The filtered supernatants were used for cleavage assays and western blotting.

Mounting fly wings

Wings from adult flies were dissected in isopropanol and mounted in Canadian Balsam mounting medium.

In situ hybridization to whole-mount embryos or discs

In situ hybridization to whole-mount embryos and wing imaginal discs was performed with digoxigenin-labeled RNA probes (visualized as a blue alkaline phosphatase precipitate) (O'Neill and Bier, 1994).

Antibody staining

Antibody staining was performed according to according to Sturtevant et al. (1993). For anti-Krüppel staining, embryos were collected from the appropriate genotypes (e.g. Table 2), aged an appropriate period of time, and fixed. We applied an anti-Krüppel antibody (1:3,000 dilution), followed by Vectastain secondary antibodies, and visualized the HRP-linked enzyme with DAB. Stained embryos were mounted in Permount or glycerol and examined and photographed using DIC optics under a compound microscope.

Injection and analysis of *Xenopus* embryos

Injection RNAs were synthesized using the mMessage mMachine kit (Ambion) according to the manufacturer's protocol provided, as described previously (Schmidt et al., 1995). 5-10 nl RNA were injected per blastomere. Embryos were injected in either 2 or 4 blastomeres of 4-cell embryos or in 1 vegetal cell at the 8-cell stage. The dorsal side of 4-cell embryos was identified by pigment and cell size differences between dorsal and ventral blastomeres at this stage. Embryos were fixed in 1× MEMFA.

RESULTS

Sog is a highly selective BMP antagonist during *Drosophila* adult development

To assess the ability of Sog to inhibit Dpp signaling in diverse developmental settings, we analyzed the effects of misexpressing Sog in various patterns during adult development. These experiments revealed that misexpression of *sog* (Table 1, Fig. 1D) or its vertebrate homologue *chordin* (Table 1, Fig. 1E) can only inhibit Dpp activity in the single adult developmental context of wing vein development to generate a phenotype very similar to that resulting from a viable combination of *gbb* alleles (Fig. 1B). Consistent with the similarities between the *gbb* loss-of-function and *sog* overexpression phenotypes, Sog can inhibit the effect of Gbb misexpression (Fig. 2D, compare with B), but not that of Dpp misexpression (Fig. 2C, compare with A). It is unlikely that the limited phenotypes resulting from Sog misexpression reflects insufficient levels of Sog expression since the same limited adult vein-loss phenotype results from low and high levels of Sog misexpression (Table 1).

Truncated forms of Sog behave as gain-of-function Dpp inhibitors

sog encodes a large protein containing four copies of a CR domain defined by the conserved spacing of ten cysteine residues (François et al., 1994) (Fig. 3). In the course of performing a structure-function analysis of the Sog protein, we identified truncated forms of Sog that generate wing phenotypes when misexpressed (Fig. 1G) similar to those of viable *dpp*⁻ mutants (Fig. 1H). We refer to such truncated forms of Sog as Supersog1, Supersog2 and Supersog4, to reflect their greater activity relative to Sog. Expression of

Table 1. Adult phenotypes resulting from misexpression of BMP antagonists

	Wing pattern							
dpp⁻ viable phenotypes	L2↔L3 L4↔L5	L3↔L4	↓P/D	Vein truncation	Cleft notum	Missing tarsae	Reduced eye size	Shortened antennae
1× *sog*	•	•	•	+[a,b]	•	•	•	•
4× *sog*	•	•	•	+[a,b]	•	•	•	•
1× *chordin*	•	•	•	+[b]	•	•	•	•
1× *follistatin*	+[b]	•	•	+[b]	•	•	•	•
1× *supersog1*	++[a,b]	+[b]	+[b]	++[a,b]	•	•	+[a]	+[a]
4× *supersog1*	+++[a,b]	++[b]	++[b]	++[a,b]	•	•	+[a]	+[a]
1× *noggin*	++[a,b]	•	+[b]	++[a,b]	+[a]	+[a]	+[a]	+[a]
4× *noggin*	+++[a,b]	•	++[b]	+++[a,b]	+[a]	+[a]	+[a]	+[a]

cDNAs encoding Dpp/BMP antagonists were misexpressed during larval and pupal development using the GAL4/UAS system (Brand and Perrimon, 1993). The *MS1096-GAL4* line drives strong ubiquitous gene expression on the dorsal surface of wing imaginal discs as well as lower levels of expression on the ventral surface (Capdevila and Guerrero, 1994), and the *dpp-GAL4* line drives gene expression in the same cells expressing *dpp*. Adult phenotypes associated with viable *dpp*⁻ loss-of-function mutations are indicated at the top and the genotypes of expressed BMP antagonists are listed below. For detailed descriptions of viable *dpp*⁻ loss-of-function mutations see Segal and Gelbart (1985). An example of a *dpp*⁻ phenotype in the wing is the moderate dpp^{d6}/dpp^{hr27} mutant (Fig. 1G).

[a]Expression of the transgene is driven by *dpp-GAL4*; [b]expression of the transgene is driven by *MS1096-GAL4*; L4<->L5 = the L4 and L5 veins are closer together or fused.

+++, extreme phenotype; ++, strong phenotype; +, moderate phenotype; •, no phenotype.

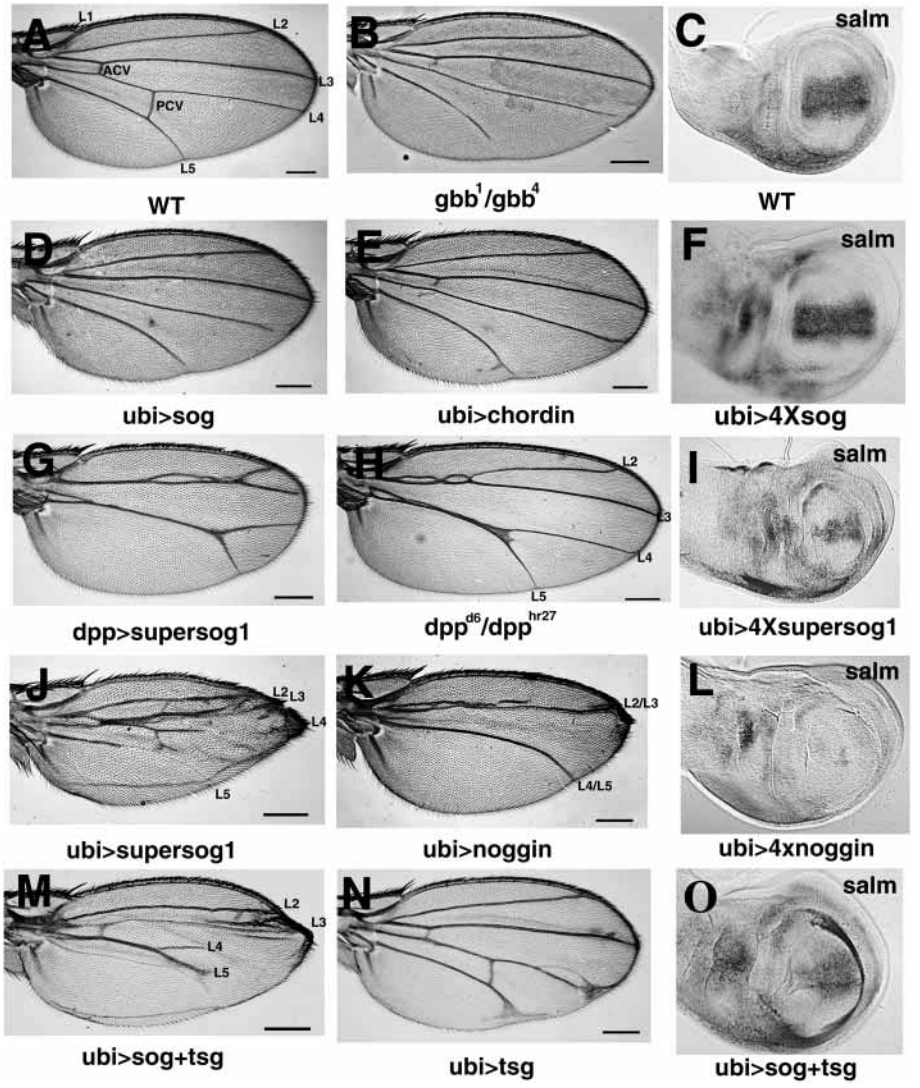

Fig. 1. Distinct activities of BMP-4 inhibitors in the *Drosophila* wing. Anterior is up and distal is to the right in all wing panels. Bars, 0.2 mm. (A) A wild-type wing. Longitudinal L1-L5 veins, the anterior cross vein (ACV) and the posterior cross vein (PCV) are labeled. (B) A wing from a fly trans-heterozygous for the *gbb1* and *gbb4* alleles. Note the similarity of this phenotype to that resulting from misexpression of *sog* or *chordin* (D,E). (C) *spalt-m (salm)* RNA expression in a wild-type wing disc. (D) Strong ubiquitous expression of *UAS-sog* results in a mild vein-loss phenotype consisting of truncation of the L4 and L5 veins at the distal tips and deletion of ACV and PCV. (E) Strong ubiquitous expression of *UAS-chordin* causes a mild vein loss-phenotype similar to that generated by *UAS-sog.* (F) *salm* expression is normal or may be slightly narrowed in an *MS1096-GAL4* > 4× *UAS*⁻ *sog* wing disc. (G) Expression of *UAS-supersog1* in *dpp* expressing cells generates a phenotype nearly indistinguishable from that of dpp^{d6}/dpp^{hr27} mutants (H). (H) A moderate viable mutant dpp^{d6}/dpp^{hr27} wing. The A/P axis is compressed and there are partial fusions of the L2 and L3 veins and the L4 and L5 veins. (I) *salm* expression is strongly reduced in an *MS1096-GAL4* > 4× *UAS- supersog1* wing disc. (J) Strong ubiquitous expression of a *UAS-supersog1* transgene generates compression along the A/P axis and vein loss. (K) Strong ubiquitous expression of *UAS-noggin* in cells comprising the dorsal surface of the wing disc (e.g. by *MS1096-GAL4*) generates A/P compression typical of dpp^{d6}/dpp^{hr27} mutants (H) and an L4 vein truncation phenotype similar to that of dpp^{shv} mutants (Segal and Gelbart, 1985). A similar phenotype is also observed using the *dpp-GAL4* driver to misexpress Noggin in cells that produce Dpp (data not shown). (L) *salm* expression is virtually eliminated in a *MS1096-GAL4* > 4× *UAS-noggin* wing disc. Similar, albeit less complete, reduction of *salm* expression is observed in *MS1096-GAL4* > 1× *UAS-noggin* wing discs (data not shown). (M) Strong ubiquitous coexpression of *UAS-sog* and *UAS-tsg* generates a strong synergistic wing phenotype similar to that observed with *UAS-supersog1* (e.g. J). (N) Strong ubiquitous expression of *UAS-tsg* causes a weak thick vein phenotype. (O) *salm* expression is severely reduced in an *MS1096-GAL4* > 1× *UAS- sog* + 1× *UAS-tsg* wing disc.

Supersog1 produces a syndrome of phenotypes characteristic of *dpp*⁻ viable mutants (Segal and Gelbart, 1985) such as small narrow wings, vein deletion, roughened and reduced eyes, and shortened antennae (Table 1). The phenotypes resulting from expression of Supersog1, Supersog2 and Supersog4 are very similar, with Supersog4 being the strongest and Supersog2 being slightly weaker than Supersog1. The activity of Supersog1 requires the presence of both the CR1 domain and the stem portion since expression of either domain alone has no effect (data not shown). In addition, Supersog molecules reduce the space between the L3 and L4 veins (Fig. 1J), a phenotype which is not observed in *dpp*⁻ mutants.

In line with the ability of misexpressed Supersog to induce phenotypes similar to those observed in *dpp*⁻ mutants, as well as additional phenotypes (e.g. reduction of the distance between the L3 and L4 veins), Supersog1 can block the effect of misexpressing both the Dpp (Fig. 2G, compare with A) and Gbb (Fig. 2H, compare with B) ligands. Supersog can block Dpp signaling upstream of the receptor, as coexpression of Supersog and an activated ligand-independent form of the Tkv receptor (Tkv*) (Fig. 2F) produces the Tkv* phenotype (Fig. 2E). Sog is similarly unable to reverse the effect of Tkv* (data not shown).

In support of the view that Supersog interferes with Dpp signaling required for establishment of the A/P axis of the wing, misexpression of Supersog1 (Fig. 1I) greatly reduces expression of the Dpp target gene *spalt major* (*salm*) in a broad central domain of the wing disc (Fig. 1C; Lecuit et al., 1996; Nellen et al., 1996; Singer et al., 1997). In contrast, identical strong misexpression of Sog has little or no effect on *salm* expression (Fig. 1F).

The observation that Supersog, but not Sog, can block the effect of Dpp misexpression and can generate a panel of *dpp*⁻ adult phenotypes could be explained either by Supersog being

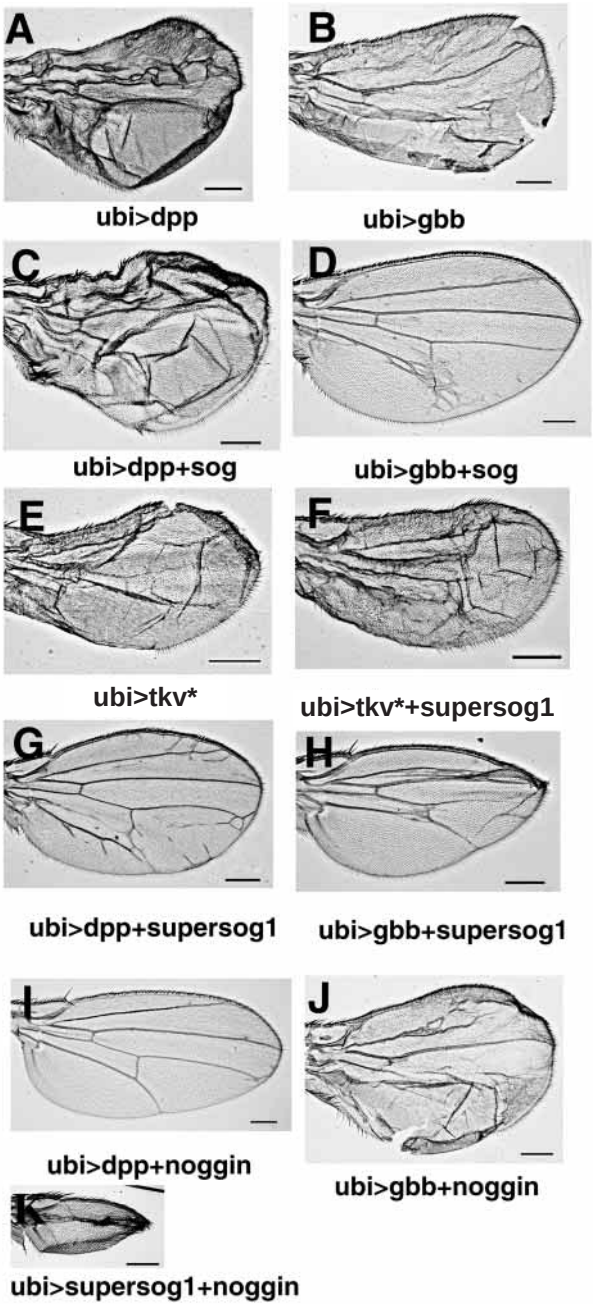

Fig. 2. BMP antagonists block the activities of different subsets of ligands. (A) Moderate ubiquitous expression of *UAS-dpp* in cells comprising the dorsal surface of the wing primordium driven by *A9-GAL4* generates broadened wings consisting of solid veins. (B) Moderate ubiquitous expression of *UAS-gbb* driven by *A9-GAL4* in cells comprising the dorsal surface of the wing primordium generates slightly broadened wings consisting of solid veins. (C) Moderate ubiquitous coexpression of *UAS-sog1* and *UAS-dpp* driven by *A9-GAL4* results in a phenotype indistinguishable from that of misexpressing *dpp* alone (compare with A). (D) Moderate ubiquitous coexpression of *UAS-sog* and *UAS-gbb* driven by *A9-GAL4* results in wings in which the solid vein phenotype resulting from *gbb* misexpression is strongly suppressed. (E) Moderate expression of *UAS-tkv** (an activated form of the Tkv receptor) driven by *A9-GAL4* results in a phenotype resembling that of *A9>UAS-dpp* (A), but does not significantly broaden the wing. (F) Moderate ubiquitous coexpression of *UAS-supersog1* and *UAS-tkv** driven by *A9-GAL4* results in a phenotype indistinguishable from that produced by expressing *UAS-tkv** alone. (G) Moderate ubiquitous coexpression of *UAS-supersog1* and *UAS-dpp* driven by *A9-GAL4* partially suppresses the broadened wing phenotype associated with *dpp* misexpression and almost completely suppresses the conversion of intervein regions into veins (compare with A). Expression of *UAS-supersog1* alone driven by *A9-GAL4* results in a phenotype similar to that shown in (H) (data not shown). (H) Moderate ubiquitous coexpression of *UAS-supersog1* and *UAS-gbb* driven by *A9-GAL4* results in wings that are virtually identical to those of flies expressing only *supersog1* (data not shown). (I) Moderate ubiquitous coexpression of *UAS-noggin* and *UAS-dpp* driven by *A9-GAL4* partially suppresses the broadened wing phenotype associated with *dpp* misexpression and almost completely suppresses the conversion of intervein regions into veins (compare with A). (J) Moderate ubiquitous coexpression of *UAS-noggin* and *UAS-gbb* driven by *A9-GAL4* results in wings that are virtually identical to those of flies expressing *gbb* alone (compare with B). (K) Strong ubiquitous coexpression of *UAS-supersog1* and *UAS-noggin* driven by *MS1096-GAL4* results in a wing of reduced size that has a fusion of all veins into a single central vein, which is a much stronger phenotype that observed with expression of either *UAS-supersog1* or *UAS-noggin* alone (compare with Fig. 1J,K). Bars, 0.2 mm.

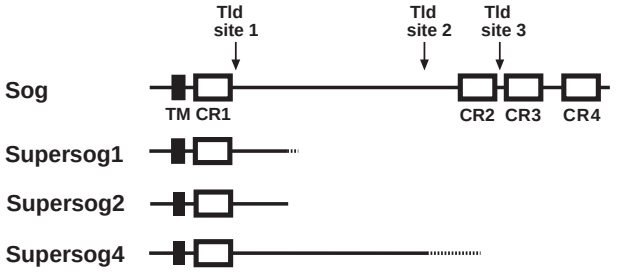

Fig. 3. Diagram of Sog constructs. The predicted Sog protein is 1038 amino acids in length and contains four cysteine-rich (CR) domains in the extracellular domain (François et al., 1994). The metalloprotease Tld cleaves Sog at three major sites indicated as Tld site 1, Tld site 2 and Tld site 3 (Marques et al., 1997). Supersog1 is an N-terminal fragment of Sog including CR1 plus another 114 amino acids, and contains an additional 33 amino acids derived from vector sequences at its C terminus (broken line). Supersog2, which contains the same amino acids as Supersog1 but terminates abruptly at the end of Sog sequences, also generates Supersog phenotypes, albeit slightly weaker than those observed with Supersog1 (data not shown). Supersog4 is an N-terminal fragment of Sog ending 80 amino acids before CR2 and includes 130 *sog* 3′ UTR derived amino acids (broken line). TM, transmembrane signal sequence.

a more potent form of Sog (e.g. have a higher affinity for the same BMP target as Sog or by being more stable) or by Supersog having gained a new function that Sog does not have. We favor the second alternative for several reasons. First, expression of one copy of Supersog generates an array of adult phenotypes never observed with four copies of Sog. Second, we find that the modest vein-loss phenotype caused by driving expression of UAS-*sog* transgenes can be observed using either strong GAL drivers (e.g. *MS1096-GAL4*) or a weaker driver (e.g. *72B-GAL4*). In contrast, when the weaker GAL4 driver is combined with UAS-*supersog* insertions, no phenotype of any kind is observed (data not shown), which indicates that it is necessary to supply more Supersog than Sog to generate the Supersog and Sog phenotypes, respectively. Similarly, in the early embryo, heat induction of 8× HS-*supersog* flies (Fig. 5F,

compare with E; see also Table 2) is less effective in inhibiting Dpp signaling in dorsalmost cells than the equivalent induction of 8× HS-*sog* embryos. Sog is also more effective than Supersog in inhibiting vein development during pupal stages (data not shown). While Supersog is more stable than Sog (e.g. it cannot be degraded by the Tld protease; see below), the fact that Supersog has less effect than Sog when expressed at equivalent moderate levels (e.g. by the *72B-GAL4* driver) argues strongly against Supersog being more potent than Sog. For these reasons, we believe that Supersog is not a higher affinity form of Sog (e.g. if anything, it is less effective than Sog on a stochiometric basis), but rather that Supersog can inhibit aspects of Dpp signaling that Sog cannot.

Vertebrate Noggin is a general inhibitor of Dpp signaling during adult development

We also tested the ability of vertebrate Noggin to inhibit Dpp signaling during adult development. As in the embryo (Holley et al., 1996), expression of Noggin in developing imaginal discs generates a nearly perfect phenocopy of the multiple defects characteristic of viable *dpp*$^{-}$ mutants (Table 1, Fig. 1K, compare with H). In addition, coexpression of Noggin with Dpp blocks the effects of overexpressing Dpp (Fig. 2I, compare with A). Noggin cannot interfere with the effect of the BMP ligand Gbb, however (Fig. 2J, compare with B).

While the phenotypes resulting from misexpressing Supersog or Noggin are quite similar overall (Table 1), Supersog causes phenotypes such as approximation of the L3 and L4 veins (Fig. 1J), which are not observed with Noggin (Fig. 1K) or in viable *dpp*$^{-}$ mutants (Fig. 1H). In addition, as mentioned above, Supersog can block the activities of both Dpp and Gbb in coexpression experiments, while Noggin can only inhibit the activity of Dpp. Consistent with Supersog and Noggin having overlapping but distinct functions, coexpression of these two BMP antagonists results in tiny wings with a single fused central vein (Fig. 2K). This phenotype reflects synergy between Supersog and Noggin as misexpression of four copies of either inhibitor alone results in phenotypes that are similar to those generated by single copies of these transgenes (data not shown). The distinct BMP inhibitory

Fig. 4. Sog is processed in vivo in a developmentally regulated fashion. (A) Immunoblot analysis of various Sog species (molecular masses indicated by arrowheads) detected with the anti-Sog-8A polyclonal antiserum directed at the amino portion of Sog. Lanes 1-3: embryonic extracts (15 embryos/lane); lanes 4,5: dissected larval wing disc extracts (45 discs/lane); lanes 6-8: dissected pupal wing extracts (20 wings/lane, except for lane 6, which contained an extract of 45 wings). 8× *HS-sog* embryos and 8× *HS-supersog1* embryos were subjected to heat shock for 30 minutes and allowed to recover at room temperature for 15 minutes before being processed for immunoblot analysis. Robust induction of the full-length 120 kDa Sog protein and lower molecular mass species migrating at 76, 42/40 and 28 kDa is observed in heat-induced early embryos (0-3 hours) (lane 2), but not in extracts from late embryo collections (6-12 hours) (lane 3). Sog bands were not detected in hand-selected pre-cellular embryos, consistent with immunohistochemical analysis (data not shown). The band migrating at approximately 28 kDa in heat-shocked 8× *HS-sog* embryos (lane 2) may correspond to a Sog product generated by Tld cleavage at site 1 immediately following CR1 (Marques et al., 1997) (Fig. 3), or may represent a secreted form of Supersog lacking the 8 kDa N-terminal type II signal sequence of Sog. Potential N-terminal fragments of Sog generated by Tld cleavage after CR1 (i.e. at site 1) would be expected to be inactive in vivo as a similarly truncated form of Sog has almost no activity when strongly expressed during adult development (data not shown). The molecular masses of abundant background bands are indicated in parentheses. Heat shocked larval wing discs produce only the full-length 120 kDa Sog band (lane 5). Little, if any, Sog protein is observed in non-heat-shocked controls (lane 4), consistent with the small proportion of wing disc cells expressing *sog* (data not shown). Lane 6 has been overloaded two- to threefold relative to other lanes. In addition to the full-length Sog band (120 kDa), heat-shocked pupal wings produce lower molecular mass N-terminal Sog bands migrating at 76, 60 and 42 kDa (lane 8). Lower, but significant levels of all of these species are observed in non-heat shocked controls (lane 7) as well as in wild-type controls that have been overloaded (lane 6), consistent with *sog* being expressed at high levels in all intervein cells during this period when it functions to suppress vein development (Yu et al., 1996). Heat shocked 8× *HS-supersog1* pupae have a doublet of bands migrating at 39/37 kDa (data not shown), which is within the range of experimental error from the predicted molecular mass of Supersog1 (36 kDa). (B) Sog is differentially cleaved in vitro by Tld in the presence of Dpp versus Tsg. Mixtures of medium (20 μl) from Sog-Myc (S) expressing cells and medium (5 μl) from Tld-HA (T) expressing cells were incubated with medium (5 μl) from Dpp-HA (D) or Tsg-His (G) expressing cells, or control medium (5 μl) for the indicated times at 25°C. Reaction products were analyzed by immunoblotting using anti-Myc antibody or amino domain 8A anti-Sog antibody. A pair of bands migrating at 42/40 kDa detected by the 8A anti-Sog antibody is produced in reaction mixes containing Sog + Tsg + Tld (S+G+T), but is not observed in mixes containing Sog + Dpp + Tld (S+D+T), Sog + Tld (S+T) or Sog + Tsg (not shown). In another control reaction (S+D+T), three Tld cleavage products of Sog migrating at 110, 55 and 35 kDa (arrowheads) were detected by anti-Myc antibody, as described before (Marques et al., 1997). The same C-terminal cleavage products are observed in reaction mixes containing Sog, Tsg and Tld (data not shown). (C) Sog and Tsg associate in vitro as revealed in a coimmune-precipitation experiment in which HA tagged Sog coprecipitates with an anti-His tagged form of Tsg. (D-F) Supersog is not degraded by activated-Tolloid in *Xenopus* embryos. (D) Embryos were injected ventrally with 2 ng *sog* RNA (top embryo) or 1 ng *supersog1* RNA (bottom embryo). Since the *sog* transcript is approximately twice the length of the *supersog1* transcript, we injected twice the amount of *sog* relative to *supersog* mRNA in order to compare equivalent molar effects of these two molecules. Injected mRNAs were synthesized using the mMessage mMachine kit (Ambion) according to the manufacturer's protocol provided as described previously (Smith and Harland, 1992). With respect to the primary axis, anterior is to the left. Embryos are at stage 34. Injection of *sog* RNA (top) or *supersog1* RNA (bottom) ventrally in *Xenopus* embryos generates a secondary axis (arrows). (E) Sog and Supersog1 induce expression of Ncam in animal caps. Embryos were injected in the animal pole with varying doses of *sog* or *supersog1* RNA as indicated, and the expression of Ncam and EF1 were assayed in animal cap explants. Lanes are as follows: lane 1, uninjected; lanes 2-5, 2.0, 1.0, 0.5 and 0.25 ng *sog* RNA, respectively; lanes 6-9, 1.0, 0.5, 0.25, 0.125 ng *supersog1* RNA, respectively. (F) Tld* inhibits secondary axis formation by Sog, but not by Supersog1. Embryos were injected ventrally with 1.5 ng *sog* RNA, 0.75 ng *supersog1* RNA and 1 ng *activated-tolloid* (*tld**) RNA, alone or in combination. Embryos were scored at stage 36 as having a 1° axis only (black bars), a 1° and 2° axis (hatched bars), or as unambiguous (white bars). All of the unambiguous embryos had the same posterior defects seen in embryos with a 2° axis. Uninjected (U), *n*=53; *sog* injected (S), *n*=28; *sog* + *tld** injected (S+T), *n*=42; *supersog1* injected (SS), *n*=40; *supersog1* + *tld** injected (SS+T), *n*=46.

activities of Sog, Supersog and Noggin indicates that these BMP antagonists block the function of differing subsets of BMPs, which collaborate to generate maximal levels of BMP signaling.

Sog is processed in vivo in a developmentally regulated fashion

To determine whether Sog might be processed in vivo to generate Supersog-like molecules, we used an anti-Sog antibody directed against an amino fragment of Sog on immunoblots to analyze protein extracts from different stages and tissues of developing *Drosophila* (Fig. 4). This antibody recognizes an epitope present in the stem portion of Supersog (data not shown). We examined the nature of Sog products produced both in wild-type individuals as well as in flies overexpressing Sog. This analysis revealed that Sog is processed in vivo, and that this processing is developmentally regulated. For example, in heat shocked early embryos carrying eight copies of an *HS-sog* construct (8× *HS-sog* flies), we observed a 76 kDa band, a doublet of bands migrating at 42/40 kDa, and a 28 kDa band (Fig. 4A, lane 2), in addition to a 120 kDa band corresponding to full-length Sog (Marques et al., 1997). These bands are likely to represent various forms of Sog since they are strongly induced only in heat shocked 8× *HS-sog* blastoderm stage embryos (compare with control in Fig. 4A, lane 1). We observed an identical pattern of inducible Sog bands using a second antiserum directed against just the CR1 domain of Sog (data not shown), indicating that these fragments, like Supersog molecules, contain both CR1 and stem domains. Similarly, heat induction of 8× *HS-sog* pupae results in the elevated production of prominent Sog fragments migrating at 76, 60, 50 and 42 kDa (Fig. 4A, lane 8; compare with lane 7). In pupal wings, the same pattern of Sog fragments is present in overloaded extracts of wild-type pupal wings (Fig. 4A, lane 6) as observed in heat induced 8× *HS-sog* wings (lane 8), albeit at lower levels. This significant level of endogenous processing is not surprising given that wild-type pupal wings express high levels of *sog* throughout intervein regions, which account for approximately 90% of cells in the wing (Yu et al., 1996).

Processing of exogenously provided Sog is developmentally regulated. During embryonic and pupal stages, when Sog is expressed in a significant fraction of cells and plays important developmental roles, distinct patterns of Sog fragments are produced. For example, during pupal development, 60, 50 and 42 kDa fragments are induced in heat shocked 8× *HS-sog* wings (Fig. 4A, lane 8), while in early embryos, a pair of induced bands migrating at 42/40 kDa is most prominent (Fig. 4A, lane 2). In contrast, during late embryonic or third larval instar stages, only the full length Sog band is observed upon induction of 8× *HS-sog* larvae (Fig. 4A, lanes 3, 5). During these latter stages of development, *sog* is expressed in only a small percentage of cells (François et al., 1994; E. Bier, unpublished observations) and is not known to have any significant developmental function. Thus, Sog is processed in vivo at developmentally relevant times and in different patterns to generate fragments that are likely to have distinct activities from Sog in addition to being degraded into inert products, as has previously been shown (Marques et al., 1997).

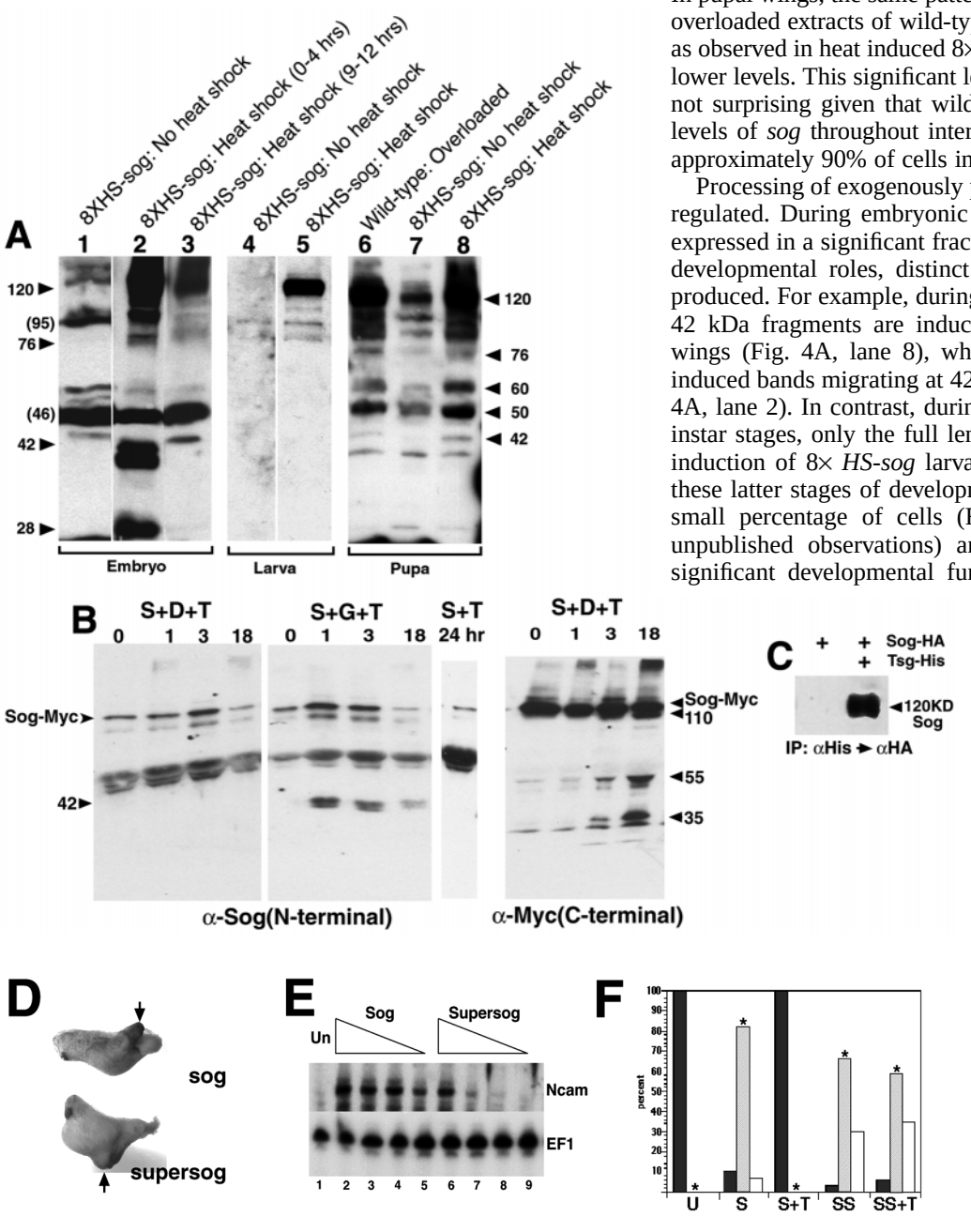

The Tld protease alters Sog processing in vitro in the presence of Tsg

One candidate protease for generating Supersog-like fragments is Tld, which has previously been shown to cleave Sog in vitro and inactivate it in *Xenopus* embryos (Marques et al., 1997). Consistent with Tld also playing a role in generating Supersog-like molecules, we

Table 2. Rescue of *tsg*⁻ and *sog*⁻ mutants by *sog* versus *supersog*

Genotype	Total number of embryos	Total number of mutant embryos	Average number of AS cells (range)
WT	25	N/A	126 (120-140)
Tsg⁻	470	68	0
sog⁻	429	48	9.1 (0-31)
4× HS-*sog*	25	N/A	107 (82-124)
4× HS-*supersog1*	25	N/A	127 (102-142)
tsg⁻;4× HS-*sog*	665	172	27.7 (14-47)
tsg⁻;4× HS-*supersog1*	600	163	74 (45-115)
sog⁻;4× HS-*sog*	472	111	83.2 (40-109)
sog⁻;4× HS-*supersog1*	355	34	47.1 (18-76)

Wild-type, *sog*[U2]/FM7c or *tsg*[N9]/FM7c mutant females indicated in the genotype column were crossed to wild type, 8× HS-*sog*, or 8× HS-*supersog1* males. Embryos from these crosses were collected over a period of 4 hours at 25°C, aged for 6 hours, fixed for immunohistochemistry, and stained for Krüppel expression in the amnioserosa as described in Materials and Methods. Mutant embryos from these collections were identified from the entire collections (Total number of embryos) based on their twisted morphology, which is a highly penetrant phenotype of *sog*⁻ and *tsg*⁻ mutant embryos. The Krüppel expressing amnioserosa cells (AS) were counted in mutant embryos (as well as in controls). These numbers are presented as the average number of AS cells and the range indicated in parentheses.

found that Tld can process Sog differently when combined with Tsg, another factor involved in Dpp signaling (Fig. 4B). Previous analysis of Tld activity revealed that three prominent carboxy-terminal cleavage products of Sog are generated when Sog, Tld and Dpp are combined (Marques et al., 1997) (Fig. 4B, lanes indicated as S+D+T). The reciprocal N-terminal degradation products of Sog are apparently unstable, however, as they could not be detected by our antibody directed at the N-terminal portion of Sog in such reactions (Fig. 4B, lanes indicated as S+D+T). In contrast, incubation of a reaction mix containing Sog, Tsg and Tld generates a prominent 42/40 kDa N-terminal processed Sog doublet in a time-dependent fashion (Fig. 4B, indicated as S+G+T, S+T). Tsg is a necessary component in this reaction as these Sog fragments are not observed in its absence (Fig. 4B, lanes S+D+T). Similar controls reveal that Tld and Sog are also required for this form of in vitro processing. These in vitro produced Sog fragments are of similar size to those generated in vivo in embryos overexpressing Sog (Fig. 4A, lane 2) and in the pupal (Fig. 4A, lanes 6, 8). The in vitro produced Sog fragments also focus on 2-D SDS-PAGE gels to the same isoelectric point as that of the Sog fragments generated from full-length Sog in embryos (data not shown), which strongly suggests that these molecules are very similar if not identical products. Tsg may alter the pattern of Tld-dependent Sog cleavage by binding to Sog since Sog coprecipitates with His-tagged Tsg (Fig. 4C). Whether Tsg alters the cleavage pattern of Tld in these experiments or acts by stabilizing an otherwise labile degradation product remains to be determined.

The ability of Tsg to alter Sog processing by Tld in vitro suggests that Tsg might promote the formation of a Supersog-like activity in vivo. In support of this possibility, coexpression of Sog and Tsg in developing wings results in a Supersog-like phenotype (Fig. 1M, compare with J), which is qualitatively different from that due to expression of Sog alone (Fig. 1D) or Tsg alone (Fig. 1N). Additionally, using *salm* as a marker for Dpp activity, we observe that coexpression of Sog and Tsg compromises *salm* expression in third instar wing discs (Fig. 1O) whereas misexpression of either *sog* (Fig. 1F) or *tsg* alone (data not shown) has little if any effect.

Supersog can partially rescue the embryonic phenotype of *tsg* mutants

In order to determine whether Sog and Tsg also interact during early embryogenesis to generate a Supersog-like activity, we compared the phenotypes of *sog* and *tsg* loss-of-function mutants. Both of these genes are expressed and function during this period to pattern the dorsal region of the embryo (François et al., 1994; Mason et al., 1994). Consistent with a previous analysis of *zen* expression (Ray et al., 1991), we observed similar patterns of expanded *rho* expression in the amnioserosa of *sog*⁻ (Fig. 5B) and *tsg*⁻ mutants (Fig. 5C). The enlarged domain of dorsal *rho* expression first becomes evident in mid-blastoderm *sog*⁻ mutant embryos, but is only observed at a later stage in *tsg*⁻ mutants as gastrulation begins. The delayed onset of amnioserosa expansion in *tsg*⁻ versus *sog*⁻ mutants suggests that *tsg* may mediate a late function of *sog*. We also observed similar patterns of *race* expression in the amnioserosa of early gastrulating *sog*⁻ and *tsg*⁻ embryos (data not shown).

The similarities in the phenotypes of *sog*⁻ and *tsg*⁻ mutants are consistent with a form of Sog (e.g. Supersog) mediating the effect of Tsg during early gastrulation. To test this hypothesis, we expressed Supersog1 during embryogenesis in wild-type and *tsg*⁻ mutant embryos and examined the expression of the amnioserosa marker Krüppel. In a wild-type background, induction of Sog expression results in a loss of early dorsal markers such as *rho*, *race* and *zen* (Biehs et al., 1996) and in a modest reduction in the final number of Krüppel expressing amnioserosa cells in late germband extended embryos (Fig. 5E, compare with D; Table 2). Similarly, expression of Supersog1 results in a small decrease in expression of early dorsal markers (data not shown) and a minor reduction in the number of Krüppel expressing cells at the germband extended stage (Fig. 5F; Table 2), which is less severe than that observed with intact Sog. Although *sog*⁻ and *tsg*⁻ mutant embryos initially show an expansion of amnioserosal markers, the final phenotype is a loss of amnioserosa (Ray et al., 1991). This paradoxical late phenotype of *sog*⁻ and *tsg*⁻ mutants may reflect the premature death of ambiguously specified amnioserosal cells, which normally undergo apoptosis later in development. We tested the possibility that a key function of Tsg might be mediated by a Supersog-like activity by expressing Supersog1 in homozygous *tsg*⁻ mutant embryos and examining the number of Krüppel expressing amnioserosa cells (Fig. 5; Table 2). In contrast to its rather weak effect in reducing the expression of dorsal markers in wild-type embryos, induction of Supersog1 expression in *tsg*⁻ mutant embryos resulted in a significant rescue of the number of Krüppel expressing cells (Fig. 5I; Table 2). By assessing the age of the partially rescued *tsg*⁻ mutant embryos (scored on the basis of their twisted morphology), we deduced that only heat shocks provided during late blastoderm stages or early gastrulation were effective in rescuing *tsg*⁻ mutants. In contrast to the potent rescuing effect of Supersog1, intact Sog had only a weak rescuing activity (Fig. 5H). We also observed rescue of *sog*⁻ mutants by Sog and Supersog1 expression, although in this case, Sog was significantly more effective than Supersog1 (Table 2). The significant rescue of *tsg*⁻ mutants by Supersog but not Sog supports the view that the function of Tsg is partly mediated by a Supersog-like activity.

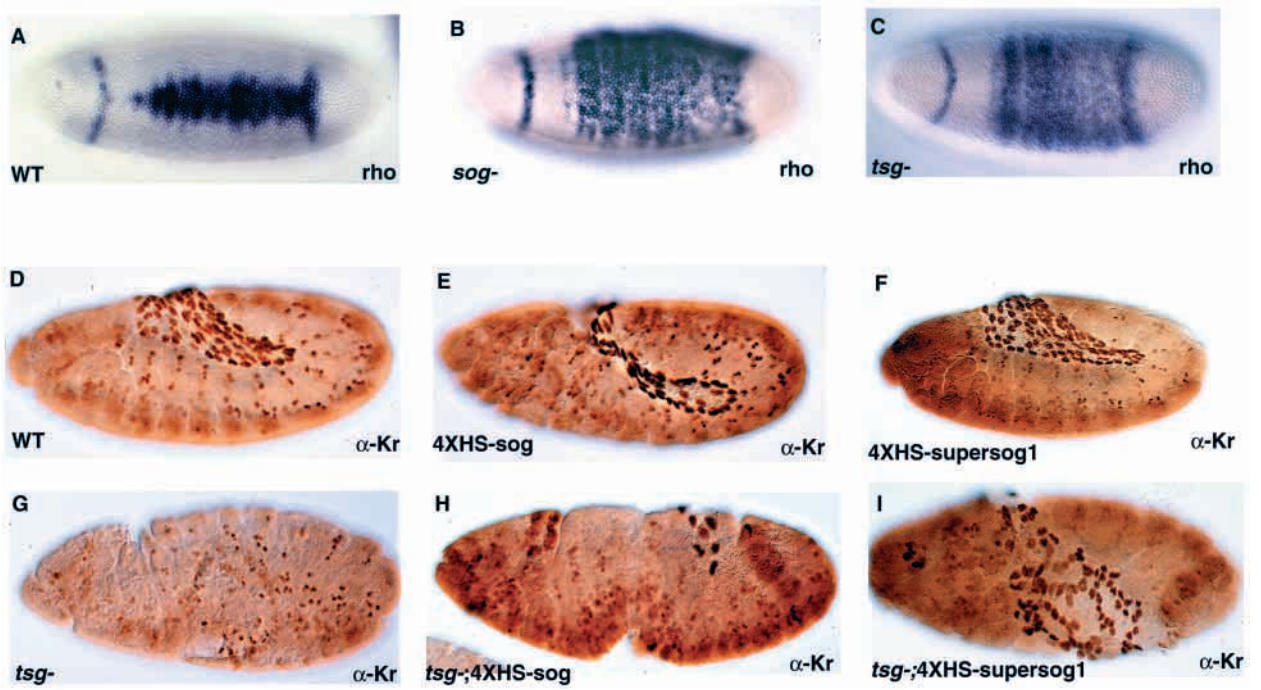

Fig. 5. Supersog partially rescues *tsg*⁻ mutants. In (A-C) the pattern of *rho* expression was determined by in situ hybridization to antisense RNA probe. (A) *rho* expression in the dorsal region of a wild-type embryo. (B) *rho* expression in the dorsal region of a *sog*⁻ mutant embryo is expanded. (C) *rho* expression in the dorsal region of a *tsg*⁻ mutant embryo is similarly expanded. In (D-I) an anti-Krüppel antibody was used to visualize the cells of the amnioserosa, which appear slightly larger than the surrounding CNS and PNS cells that also express Krüppel. (D) Krüppel expression in a wild-type embryo. (E) The number of Krüppel expressing cells is slightly reduced in 4× HS-*sog* embryos relative to wild type. (F) The number of Krüppel expressing cells is indistinguishable from wild type in 4× HS-*supersog1* embryos. (G). There are no Krüppel expressing amnioserosa cells in *tsg*⁻ embryos. (H) The number of Krüppel expressing amnioserosa cells in *tsg*⁻; 4× HS-*sog* embryos that received heat shocks during late blastoderm stages is increased slightly over that observed in non-heat induced embryos. (I) Heat shocking *tsg*⁻; 4× HS-*supersog-1* embryos results in significant rescue of Krüppel expressing amnioserosal cells.

Supersog is immune to degradation by Tld in *Xenopus* embryos

Since an activated form of the Tld protease (Tld*) can cleave and inactivate Sog in a *Xenopus* double axis assay (Marquez et al., 1997), we wondered whether Supersog likewise could be inactivated by Tld*. As in the case of Sog (Holley et al., 1995; Schmidt et al., 1995), injection of *supersog1* mRNA into *Xenopus* embryos induces the formation of a secondary axis (Fig. 4D) and expression of the neural marker Ncam (Fig. 4E). However, in contrast to wild-type Sog (Marques et al., 1997), the effects of Supersog1 cannot be reversed by coinjection of Tld* (Fig. 4F). The resistance of Supersog1 to degradation by Tld may contribute to its broadened activity relative to Sog. As mentioned above, however, increased stability or levels of Supersog versus Sog cannot alone account for the fact that moderate or high levels of Sog expression generate the same mild wing vein phenotypes while moderate levels of Supersog expression generate no detectable phenotype of any kind.

DISCUSSION

BMP antagonists have distinct activities

Data presented in this study suggest that differential processing of Sog generates molecules with distinct effects on BMP signaling. Sog and Supersog define nearly opposite poles of the specificity spectrum since during adult development, Sog only inhibits BMP signaling in the context of wing vein development, while Supersog, like Noggin, inhibits a broad range of BMP signaling events. One way to explain the variety of phenotypes induced by misexpressing different BMP antagonists is that the various forms of Sog and structurally diverse BMP antagonists recognize partially non-overlapping subsets of BMP targets. Consistent with this model, we observe that Sog, Supersog and Noggin suppress the misexpression effects of different subsets of known BMPs acting in the wing. Thus, Sog only suppresses the action of Gbb, Supersog blocks both Gbb and Dpp, and Noggin only blocks Dpp. The synergistic interactions we observe among BMP antagonists also strongly suggest that these inhibitors recognize partially non-overlapping subsets of BMP targets. This diversity of function of BMP antagonists provides some insight into why the Spemann organizer secretes a cocktail of diverse BMP binding factors such as Chordin, Noggin and Follistatin. These BMP antagonists may exert distinct functions, as has been observed during dorsal-ventral patterning of the vertebrate neural tube (Liem et al., 1997). Cumulatively, our results strongly suggest that neural inducing BMP antagonists play distinct roles in regulating the quality as well as magnitude of BMP signaling.

Sog is processed in vivo in a developmentally regulated fashion

We present evidence that Sog is processed in vivo to generate N-terminal fragments which overlap with Supersog molecules.

Sog can be processed to generate a distinct pattern of fragments in early embryos. Endogenous Sog is also likely to be processed in wild-type pupal wings since overexpression of Sog during pupal development gives rise to increased levels of Sog fragments, which are present in wild-type wings. Sog processing is likely to be developmentally regulated, since overexpression of Sog during early embryonic and pupal development, when Sog normally contributes to patterning, generates similar but distinct patterns of Sog processing. In contrast, Sog is not detectably processed in late embryos or larvae, which are stages of development when Sog has no apparent function and when overexpression of Sog results in no phenotype. The finding that Sog harbors cryptic functions suggests that Sog and Chordin, which are modular proteins several times larger than Noggin or Follistatin, may have more dynamic and varied roles in modulating BMP signaling than the smaller dedicated BMP antagonists.

The Tld protease cleaves Sog to generate a Supersog-like activity in the presence of Tsg

It has previously been shown that the metalloprotease Tld can cleave Sog in vitro and that addition of Tld to Sog can reverse the ability of Sog to generate a double axis in *Xenopus* embryos (Marques et al., 1998). These results are consistent with the D/V patterning defects observed in *tld* overexpress mutants, which resemble those associated with partial loss-of-function *dpp*$^-$ mutants (Wharton et al., 1993). The data reported in this paper demonstrate that the pattern of Sog cleavage by Tld can be radically altered by addition of Tsg, another secreted product involved in early D/V patterning of *Drosophila* embryos. The size of the N-terminal Sog fragments produced by Tld + Tsg in vitro is very close to processed Sog fragments generated in vivo in early embryos and in pupal wings. Since the in vitro products also have the same isoelectric point as those produced from intact Sog in early embryos, it is likely that these molecules are very similar if not identical. Consistent with the Tsg dependent Sog processing being relevant in vivo, combined expression of Sog and Tsg creates a Supersog-like wing phenotype and leads to suppression of Dpp signaling in wing imaginal discs. As *tld* and the *tolloid-related* gene are both broadly expressed during larval development (Nguyen et al., 1994), Tsg or related proteins may be the key factors required for Sog processing that are missing during this stage. The fact that *tld* and *tsg*, two genes known to be involved in Dpp signaling, collaborate to generate a Supersog-like product in vivo and in vitro strongly supports the view that the Sog processing we observe in vivo is biologically meaningful. Furthermore, the similar phenotypes of *sog*$^-$ and *tsg*$^-$ mutant embryos and the ability of Supersog1, but not full-length Sog, to provide significant rescue of the *tsg*$^-$ embryonic phenotype suggests that a Supersog-like activity mediates a key component of *tsg* function. In addition to the 40/42 kDa forms of Sog which are generated in vitro and in vivo in early embryos and pupae, several higher molecular weight Sog bands are generated in pupae. One of these forms (the 60 kDa species) is also generated during oogenesis (H. Araujo and E. B., unpublished). Whether Tld/Tld-related or some other type of protease are involved in the production of these alternative forms of Sog remains to be determined.

Although the combined in vivo and in vitro data are all consistent with a Supersog-like processed form of Sog being produced and having a developmental function, we cannot rule out an alternative possibility that the active form of Sog is actually uncleaved Sog bound to Tsg. According to this scenario, differential Sog processing would be a secondary consequence of a conformational change in Sog brought about by binding to Tsg, which would unfold Sog making the CR1 domain available to interact with other BMPs such as Dpp. Truncation of Sog would mimic the formation of such an extended Sog-Tsg complex, perhaps by eliminating a negative regulatory interaction between the CR2-CR4 domains and CR1. Distinguishing between these two possibilities will require additional analysis.

As Sog processing is developmentally controlled, it is tempting to speculate that regulation of genes encoding proteases like Tld and cofactors such as Tsg may determine the nature of Sog fragments produced in different developmental contexts. These various forms of Sog may have distinct functions from Sog and Supersog since we have evidence for the existence of additional Sog activities beyond those provided by Sog and Supersog (K. Yu et al., S. Srinivasan et al., unpublished). For example, one form of Sog appears to promote rather than inhibit Dpp activity, consistent with recent genetic evidence for a long-range Sog activity that enhances Dpp signaling (Ashe and Levine, 1999). We note that differential processing of large protein precursor molecules such as the proopiomelanocortin precursor (POMC) in different cells of the pituitary is a well known and effective mechanism for producing a diversity of peptide functions from one gene product (Castro and Morrison, 1997). Analogous mechanisms regulating Sog processing in different cells may play important regulatory roles in shaping the response of individual cells to particular combinations of BMPs during development.

Mechanisms by which Sog products may modulate BMP signaling

As mentioned above, we find that Sog and Supersog have distinct effects when misexpressed in the wing. In particular, Supersog, but not Sog, can inhibit Dpp signaling during A/P patterning of the wing imaginal disk. Whether the documented function of Sog during vein development (Yu et al., 1996) results from the activity of intact Sog or one of the several Sog fragments produced in pupal wings remains to be determined, since both Sog and Supersog can inhibit vein formation when misexpressed during pupal wing development (although Sog is somewhat more effective than Supersog during this period). We also find that structurally unrelated proteins such as Noggin and Follistatin (data not shown) cause different wing phenotypes. One way to explain the effect of Sog, Supersog molecules and other BMP antagonists is to hypothesize that they intercept different subsets of BMP family members. The observation that Supersog1 functions upstream of the Tkv receptor is consistent with this type of mechanism. Also, we observe that Sog can inhibit the function of Gbb but not Dpp during wing development. Likewise, it has recently been reported that Sog inhibits the action of Screw, but not Dpp in the early embryo (Neul and Ferguson, 1998; Nguyen et al., 1998). The ability of Supersog to block the action of Dpp as well as Gbb is consistent with the possibility that Supersog recognizes both Gbb and Dpp. However, Supersog is likely to inhibit the function of at least one additional BMP target, since misexpression of

Supersog can reduce the space between the L3 and L4 veins, which is not caused by reduction of *dpp* or *gbb* gene function or misexpression of Noggin. Additional evidence for Supersog interfering with a signal other than Dpp is that coexpression of Supersog with Noggin results in synergistic rather than additive effects, whereas coexpression of Sog and Noggin results in only a Noggin-like phenotype (K. Yu, unpublished observation). An alternative possibility is that Supersog binds to other extracellular components of the BMP signaling pathway such as BMP-receptors. In this model Supersog would prevent BMPs from gaining access to their receptors or would interfere with the formation of higher order receptor-ligand complexes necessary for maximal signaling activity. Determining the mechanism(s) by which Supersog functions is an important question to address in future experiments.

Possible biological functions of a Supersog-like activity

The fact that pulses of Supersog1 expression delivered during the late blastoderm stage of development can partially rescue the *tsg*$^-$ mutant embryos suggests that a Supersog-like activity might mediate part of *tsg* function in vivo. In addition, late blastoderm stage *tsg*$^-$ mutant embryos display defects similar to those of *sog* mutants, suggesting that *tsg* is involved in a late function of Sog. Consistent with the view that *tsg* acts during early gastrulation, Mason et al. (1994) noted that *tsg*$^-$ mutants could not be rescued by driving expression of a *tsg* transgene under the control of the *tld* promoter, which is expressed only early during the blastoderm stage. In contrast, these authors found that it was possible to rescue *tsg*$^-$ mutants by driving *tsg* expression with promoters that continue to be expressed into early gastrulation. We can imagine several possible ways in which Supersog-like activities could contribute to this stage of development, given that they have different ligand specificities from intact Sog and are stable to further proteolysis by Tld. Since Sog has been proposed to block the activity of Scw in embryos, it is likely that some other BMP is the preferred target of Supersog molecules. In addition, since Scw is only expressed transiently during the blastoderm stage of development, intact Sog would have no obvious target to inhibit beyond this stage. Perhaps a stable broad-spectrum BMP antagonist such as Supersog could inhibit the action of other BMPs expressed in the dorsal ectoderm during early stages of gastrulation (possibly Dpp itself) and thereby provide a form of molecular memory, which helps maintain the distinction between neural and non-neural ectoderm.

The observation that Supersog is less effective than Sog in blocking BMP signaling in the early embryo is consistent with the view that Supersog is not just a higher affinity version of Sog and suggests that Supersog is actually less effective than Sog at blocking the effect of Scw. The fact that Supersog does not inhibit Dpp itself during early blastoderm stages is likely to be the result of insufficient levels of Supersog being expressed by the heat shock vector. It is possible, however, that an endogenously produced Supersog activity (e.g. generated upon Tsg binding to Sog) has a higher affinity for Dpp than the artificially created Supersog1 construct. In any case, we propose that Supersog acts in the late blastoderm embryo or during early gastrulation stages rather than in the early blastoderm embryo, and that during this latter period, it is able to block the activity of a BMP (e.g. Dpp?) not recognized by Sog.

It is tempting to consider a two step temporal model for the action of Sog and Supersog during embryonic dorsal-ventral patterning to account for the fact that *sog* mutants display a dorsal-ventral phenotype earlier than *tsg*$^-$ mutants. According to one such scenario, the labile Tld-sensitive form of full-length Sog is produced from a localized source (i.e. the neuroectoderm) and diffuses dorsally to be degraded by Tld. Tld acts as a sink to create a transiently stable gradient of Sog, which creates a reciprocal gradient of Dpp activity. The Sog gradient created by this classic source/sink configuration would only be short-lived, however, since cells begin migrating when gastrulation begins. At this stage, the embryo elongates and the Dorsal gradient collapses, leading to loss of gene expression in early zygotic D/V domains. Following the establishment of the short-lived hypothetical Sog gradient, *tsg* expression is initiated in dorsal cells and leads to the production of stable Supersog-like molecules by switching the activity of Tld from degrading to activating Sog. Supersog-like molecules then could provide a stable record of high versus low BMP signaling domains during a subsequent step of development.

Future experiments will be required to assign specific functions to the various forms of Sog that are produced at different stages of development.

We thank Michael Hoffmann for providing the anti-Sog antibody, Larry Marsh and Liz Mason for a *tsg* cDNA and for UAS-*tsg* lines, Chris Kintner for providing the *pGEM5-noggin* construct, Dan Ang for microinjecting P-element constructs into *Drosophila* embryos, Hank Farr for assistance in injecting various mRNAs into *Xenopus* embryos, and Steve Wasserman for suggesting the experiment of rescuing *tsg*$^-$ mutants with Supersog.

REFERENCES

Arora, K. and Nüsslein-Volhard, C. (1992). Altered mitotic domains reveal fate map changes in *Drosophila* embryos mutant for zygotic dorsoventral patterning genes. *Development* **114**, 1003-1024.

Arora, K., Levine, M. S. and O'Connor, M. B. (1994). The *screw* gene encodes a ubiquitously expressed member of the TGF-β family required for specification of dorsal cell fates in the *Drosophila* embryo. *Genes Dev* **8**, 2588-2601.

Ashe, H. L. and Levine, M. (1999). Local inhibition and long-range enhancement of Dpp signal transduction by Sog. *Nature* **398**, 427-431.

Biehs, B., François, V. and Bier, E. (1996). The *Drosophila short gastrulation* gene prevents Dpp from autoactivating and suppressing neurogenesis in the neuroectoderm. *Genes Dev.* **10**, 2922-2934.

Bier, E. (1997). Anti-neural-inhibition, a conserved mechanism for neural induction. *Cell* **89**, 681-684.

Brand, A. H. and Perrimon, N. (1993). Targeted gene expression as a means of altering cell fates and generating dominant phenotypes. *Development* **118**, 401-415.

Bunch, T. A., Grinblat, Y. and Goldstein, L. S. B. (1988). Characterization and use of the *Drosophila* metallothionein promoter in cultured *Drosophila melanogaster* cells. *Nucleic Acids Res.* **16**, 1043-1061.

Campbell, G., Weaver, T. and Tomlinson, A. (1993). Axis specification in the developing *Drosophila* appendage, the role of *wingless*, *decapentaplegic*, and the homeobox gene *aristaless*. *Cell* **74**, 1113-1123.

Capdevila, J. and Guerrero, I. (1994). Targeted expression of the signaling molecule *decapentaplegic* induces pattern duplications and growth alterations in *Drosophila* wings. *EMBO J.* **13**, 4459-4468.

Castro, M. G. and Morrison, E. (1997). Post-translational processing of proopiomelanocortin in the pituitary and in the brain. *Crit. Rev. Neurobiol.* **11**, 35-57.

Chen, Y., Riese, M. J., Killinger, M. A. and Hoffmann, F. M. (1998). A genetic screen for modifiers of *Drosophila decapentaplegic* signaling identifies mutations in *punt*, *Mothers against Dpp*, and the BMP-7 homologue *60A*. *Development* **125**, 1759-1768.

Ferguson, E. L. and Anderson, K. V. (1992). Localized enhancement and repression of the activity of the TGF-β family member, *decapentaplegic*, is necessary for dorsal-ventral pattern formation in the *Drosophila* embryo. *Development* **114**, 583-597.

François, V. and Bier, E. (1995). The *Xenopus chordin* and the *Drosophila short gastrulation* genes encode homologous proteins functioning in dorsal-ventral axis formation. *Cell* **80**, 19-20.

François, V., Solloway, M., O'Neill, J. W., Emery, J. and Bier, E. (1994). Dorsal-ventral patterning of the *Drosophila* embryo depends on a putative negative growth factor encoded by the *short gastrulation* gene. *Genes Dev.* **8**, 2602-2616.

Frasch, M. (1995). Induction of visceral and cardiac mesoderm by ectodermal Dpp in the early *Drosophila* embryo. *Nature* **374**, 464-467.

Haerry, T. E., Khalsa, O., O'Connor, M. B. and Wharton, K. A. (1998). Synergistic signaling by two BMP ligands through the SAX and TKV receptors controls wing growth and patterning in *Drosophila*. *Development* **125**, 3977-3987.

Hammerschmidt, M., Serbedzija, G. N. and McMahon, A. P. (1996). Genetic analysis of dorsoventral pattern formation in the zebrafish, requirement of a BMP-like ventralizing activity and its dorsal repressor. *Genes Dev.* **10**, 2452-2461.

Han, K. (1996). An efficient DDAB-mediated transfection of *Drosophila* S2 cells. *Nucleic Acids Res.* **24**, 4362-4363.

Heberlein, U., Wolff, T. and Rubin, G. M. (1993). The TGF beta homolog *dpp* and the segment polarity gene *hedgehog* are required for propagation of a morphogenetic wave in the *Drosophila* retina. *Cell* **75**, 913-926.

Hemmati-Brivanlou, A. and Melton, D. A. (1997). Vertebrate embryonic cells will become nerve cells unless told otherwise. *Cell* **88**, 13-17.

Holley, S. A., Jackson, P. D., Sasai, Y., Lu, B., De Robertis, E. M., Hoffmann, F. M. and Ferguson, E. L. (1995). A conserved system for dorsal-ventral patterning in insects and vertebrates involving *sog* and *chordin*. *Nature* **376**, 249-253.

Holley, S. A., Neul, J. L., Attisano, L., Wrana, J. L., Sasai, Y., O'Connor, M. B., De Robertis, E. M. and Ferguson, E. L. (1996). The *Xenopus* dorsalizing factor *noggin* ventralizes *Drosophila* embryos by preventing DPP from activating its receptor. *Cell* **86**, 607-617.

Hursh, D. A., Padgett, R. W. and Gelbart, W. M. (1993). Cross regulation of *decapentaplegic* and *Ultrabithorax* transcription in the visceral mesoderm of *Drosophila*. *Development* **117**, 1211-1222.

Irish, V. F. and Gelbart, W. M. (1987). The *decapentaplegic* gene is required for dorsal-ventral patterning of the *Drosophila* embryo. *Genes Dev.* **1**, 868-879.

Kaphingst, K. and Kunes, S. (1994). Pattern formation in the visual centers of the *Drosophila* brain, *wingless* acts via *decapentaplegic* to specify the dorsoventral axis. *Cell* **78**, 437-448.

Khalsa, O., Yoon, J. W., Torres-Schumann, S. and Wharton, K. A. (1998). TGF-beta/BMP superfamily members, Gbb-60A and Dpp, cooperate to provide pattern information and establish cell identity in the *Drosophila* wing. *Development* **125**, 2723-2734.

Lecuit, T., Brook, W. J., Ng., M., Calleja, M., Sun, H. and Cohen, S. M. (1996). Two distinct mechanisms for long range patterning by Decapentaplegic in the *Drosophila* wing. *Nature* **381**, 387-393.

Liem, K. F., Jr, Tremml G. and Jessell, T. M. (1997). A role for the roof plate and its resident TGFβ-related proteins in neuronal patterning in the dorsal spinal cord. *Cell* **91**, 127-138.

Ma, C. Y., Beachy, P. A. and Moses, K. (1993). The segment polarity gene *hedgehog* is required for progression of the morphogenetic furrow in the developing *Drosophila* eye. *Cell* **75**, 927-938.

Marques, G., Musacchio, M., Shimell, M. J., Wunnenberg, S. K., Cho, K. W. and O'Connor, M. B. (1997). Production of a DPP activity gradient in the early *Drosophila* embryo through the opposing actions of the SOG and TLD proteins. *Cell* **91**, 417-426.

Mason, E. D., Konrad, K. D., Webb, C. D. and Marsh, L. J. (1994). Dorsal midline fate in *Drosophila* embryos requires *twisted gastrulation*, a gene encoding a secreted protein related to human connective tissue growth factor. *Genes Dev.* **8**, 1489-1501.

Mason, E. D., Williams, S., Grotendorst, G. R. and Marsh, L. J. (1997). Combinatorial signaling by Twisted Gastrulation and Decapentaplegic. *Mech. Dev.* **64**, 61-75.

Nellen, D., Burke, R., Struhl, G. and Basler, K. (1996). Direct and long-range action of a DPP morphogen gradient. *Cell* **85**, 357-368.

Neul, J. L. and Ferguson, E. L. (1998). Spatially restricted activation of the SAX receptor by SCW modulates DPP/TKV signaling in *Drosophila* dorsal-ventral patterning. *Cell* **95**, 483-494.

Nguyen, T., Jamal, J., Shimell, M. J., Arora, K. and O'Connor, M. B. (1994). Characterization of tolloid-related-1, a BMP-1-like product that is required during larval and pupal stages of *Drosophila* development. *Dev. Biol.* **166**, 569-586.

Nguyen, M., Park, S., Marques, G. and Arora, K. (1998). Interpretation of a BMP activity gradient in Drosophila embryos depends on synergistic signaling by two type I receptors, SAX and TKV. *Cell* **95**, 495-506.

O'Neill, J. W. and Bier, E. (1994). Double label in situ hybridization using biotin and digoxigenin tagged RNA probes. *BioTechniques* **17**, 870-875.

Padgett, R. W., St Johnson, R. D. and Gelbart, W. M. (1987). A transcript from a *Drosophila* pattern gene predicts a protein homologous to the transforming growth factor-β family. *Nature* **325**, 81-84.

Padgett, R. W., Wozney, J. M. and Gelbart, W. M. (1993). Human BMP sequences can confer normal dorsal-ventral patterning in the *Drosophila* embryo. *Proc. Natl. Acad. Sci. USA* **90**, 2905-2909.

Panganiban, G. E., Reuter, R., Scott, M. P. and Hoffmann, F. M. (1990). A *Drosophila* growth factor homolog, *decapentaplegic*, regulates homeotic gene expression within and across germ layers during midgut morphogenesis. *Development* **110**, 1041-1050.

Piccolo, S., Sasai, Y., Lu, B. and De Robertis, E. M. (1996). Dorsoventral patterning in *Xenopus*, inhibition of ventral signals by direct binding of Chordin to BMP-4. *Cell* **86**, 589-598.

Ray, R. P., Arora, K., Nüsslein-Volhard, C. and Gelbart, W. M. (1991). The control of cell fate along the dorsal-ventral axis of the *Drosophila* embryo. *Development* **113**, 35-54.

Sasai, Y., Lu, B., Steinbeisser, H. and De Robertis, E. M. (1995). Regulation of neural induction by the Chd and Bmp-4 antagonistic patterning signals in *Xenopus*. *Nature* **376**, 333-336.

Sasai, Y., Lu, B., Steinbeisser, H., Geissert, D., Gont, L. K. and De Robertis, E. M. (1994). *Xenopus chordin*, a novel dorsalizing factor activated by organizer-specific homeobox genes. *Cell* **79**, 779-790.

Schmidt, J., François, V., Bier, E. and Kimelman, D. (1995). *Drosophila short gastrulation* induces an ectopic axis in *Xenopus*, evidence for conserved mechanisms of dorsal-ventral patterning. *Development* **121**, 4319-4328.

Segal, D. and Gelbart, W. M. (1985). *shortvein*, a new component of the *decapentaplegic* gene complex in *Drosophila melanogaster*. *Genetics* **109**, 119-143.

Singer, M. A., Penton, A., Twombly, V., Hoffmann, F. M. and Gelbart, W. M. (1997). Signaling through both type I Dpp receptors is required for anterior-posterior patterning of the entire *Drosophila* wing. *Development* **124**, 79-89.

Smith, W. C. and Harland, R. M. (1992). Expression cloning of *noggin*, a new dorsalizing factor localized to the Spemann organizer in *Xenopus* embryos. *Cell* **70**, 829-840.

Staehling-Hampton, K., Hoffmann, F. M., Baylies, M. K., Rushton, E. and Bate, M. (1994). *dpp* induces mesodermal gene expression in *Drosophila*. *Nature* **372**, 783-786.

Sturtevant, M. A., Roark, M. and Bier, E. (1993). The *Drosophila rhomboid* gene mediates the localized formation of wing veins and interacts genetically with components of the Egf-R signaling pathway. *Genes Dev.* **7**, 961-973.

Thuringer, F., Cohen, S. M. and Bienz, M. (1993). Dissection of an indirect autoregulatory response of a homeotic *Drosophila* gene. *EMBO J.* **12**, 2419-2430.

Twombly, V., Blackman, R. K., Jin, H., Graff, J. M., Padgett, R. W. and Gelbart, W. M. (1996). The *decapentaplegic* signalling pathway is essential for *Drosophila* oogenesis. *Development* **122**, 1555-1565.

Wappner, P., Gabay, L. and Shilo, B. Z. (1997). Interactions between the EGF receptor and DPP pathways establish distinct cell fates in the tracheal placodes. *Development* **124**, 4707-4716.

Wharton, K. A., Ray, R. P. and Gelbart, W. M. (1993). An activity gradient of *decapentaplegic* is necessary for the specification of dorsal pattern elements in the *Drosophila* embryo. *Development* **117**, 807-822.

Wilson, P. A. and Hemmati-Brivanlou, A. (1995). Induction of epidermis and inhibition of neural fate by Bmp-4. *Nature* **376**, 331-333.

Yu, K., Sturtevant, M. A., Biehs, B., François, V., Padgett, R. W., Blackman, R. K. and Bier, E. (1996). The *Drosophila decapentaplegic* and *short gastrulation* genes function antagonistically during adult wing vein development. *Development* **122**, 4033-4044.

Zimmerman, L. B., De Jesus-Escobar, J. and Harland, R. M. (1996). The Spemann organizer signal Noggin binds and inactivates Bone Morphogenetic Protein 4. *Cell* **86**, 599-606.